The Astrophysical Journal, 591:283–287, 2003 July 1

DELAYED FLASHES FROM COUNTERJETS OF GAMMA-RAY BURSTS

Ryo Yamazaki
Department of Physics, Kyoto University, Kyoto 606-8502, Japan; yamazaki@tap.scphys.kyoto-u.ac.jp

Kunihito Ioka
Department of Earth and Space Science, Osaka University, Toyonaka 560-0043, Japan; ioka@vega.ess.sci.osaka-u.ac.jp

and

Takashi Nakamura
Department of Physics, Kyoto University, Kyoto 606-8502, Japan; takashi@tap.scphys.kyoto-u.ac.jp
Received 2002 July 27; accepted 2003 March 6

ABSTRACT

If X-ray flashes are due to the forward-jet emissions from gamma-ray bursts (GRBs) observed at large viewing angles, we show that a prompt emission from a counterjet should be observed as a "delayed flash" in the UV or optical band several hours to a day after the X-ray flash. The Ultraviolet and Optical Telescope on *Swift* can observe the delayed flashes within ~13 Mpc, so that (double-sided) jets of GRBs can be directly confirmed. Since the event rate of delayed flashes detected by *Swift* may be as small as $\sim 6 \times 10^{-5}$ events yr^{-1}, we require more sensitive detectors in future experiments.

Subject headings: gamma rays: bursts — gamma rays: theory

1. INTRODUCTION

Several observations suggest that gamma-ray bursts (GRBs) are caused by relativistic jets (e.g., Frail et al. 2001). However, in order to establish that GRBs are collimated, other observations are indispensable, such as polarization observations (Ghisellini & Lazzati 1999; Sari 1999) and microlensing observations (Ioka & Nakamura 2001b). Some theoretical models of jet emissions have been discussed (Totani & Panaitescu 2002; Huang, Dai, & Lu 2002; Dado, Dar, & De Rújula 2002). If GRBs are due to forward-jet emissions, there should most likely be counterjet emissions, as in the active galactic nucleus (AGN; Begelman, Blandford, & Rees 1984) and the microquasar (Mirabel & Rodríguez 1999). Therefore, the detection of counterjet emissions will give us direct evidence for the jet model of GRBs.

The confirmation of a counterjet has been by far the most important factor in the jet model of astrophysical objects. A mysterious spot was found in SN 1987A using the speckle technique (Meikle et al. 1987; Nisenson et al. 1987). Many models including the jet model were proposed (Rees 1987; Piran & Nakamura 1987). At that time, it was difficult to distinguish each model by observation, since only one spot was found. In the jet model, the counterjet should be observed, although it would be dim because of redshifting (Piran & Nakamura 1987). However, later in 1999, two spots were confirmed using new software to analyze the speckle data (Nisenson & Papaliolios 1999). Very recently, the jet feature of the ejecta of SN 1987A, whose position angle is the same as the mysterious spot, was confirmed by the *Hubble Space Telescope* (Wang et al. 2002). As a result, the jet model by Piran & Nakamura (1987) took the advantage. Furthermore, the observation of a counterjet may enable us to estimate the Lorentz factor of the jet, as for the AGN and microquasar. Therefore, it is important to discuss the observational properties of the emission from the counterjet of a GRB.

Let us consider the emission from a counterjet with a Lorentz factor γ. The observed typical frequency of the counterjet emission is about γ^2 times smaller than that of the forward jet (i.e., the GRB). Since the typical frequency of the GRB is ~100 keV, the typical observed frequency of the counterjet emission is $\sim 10(\gamma/100)^{-2}$ eV, which is in the UV or optical band. This transient phenomenon should be observed about several tens of hours after the forward-jet emission, since it is at a radius of the order of 10^{14}–10^{15} cm that photons are emitted from each jet leaving, almost simultaneously, the central engine. We call this event the "delayed flash" (DF).

Any attempt to detect the DF might be difficult since the afterglow of the forward jet might be brighter than the DF. The afterglow of the GRB, i.e., the afterglow of the on-axis forward jet, is much brighter than the DF. However, if the forward jet is observed with a large viewing angle, there is a chance to observe the DF, since the forward-jet emission is also dim at the time of the DF.

Recently, we studied the emission from an off-axis jet (Yamazaki, Ioka, & Nakamura 2002a, 2002b; see also Nakamura 2000; Ioka & Nakamura 2001a). We proposed that if we observe a GRB with a large viewing angle, it looks like an X-ray flash (XRF), a new class of X-ray transients that has been recently recognized as a phenomenon related to the GRB (e.g., Heise et al. 2001; Kippen et al. 2003; Barraud et al. 2003). The off-axis jet model can explain the typical observed frequency and other observational characteristics of the XRF, such as the peak flux ratio, the fluence ratio between the gamma-ray and the X-ray band, the X-ray photon index, the typical duration, and the event rate (Yamazaki, Ioka, & Nakamura 2002a, 2002b). Although the origin of XRFs is uncertain, we assume that XRFs arise from prompt off-axis jet emissions hereafter.

In this paper we show that the DF can be observed after the XRF in principle. We calculate the light curves of the XRF, DF, and the afterglow of the XRF and discuss whether the DF can be detected by the *Swift* satellite. We find that we need more sensitive detectors to detect the DF. In § 2 we describe a simple forward/counterjet model for the XRF and DF. In §§ 3 and 4 we show the light curves of the XRF, the DF, and the XRF afterglow. Section 5 is devoted to a discussion.

2. INSTANTANEOUS EMISSION FROM AN EXPANDING JET

We extend the simple jet model by Ioka & Nakamura (2001a) and Yamazaki, Ioka, & Nakamura (2002a). In these works we assume that the shell width l is much smaller than the separation of the shells L in the internal shock, since the separation L mainly determines the emission timescale of the forward jet. However, in this paper we consider a finite shell width, since the shell width l determines the emission timescale of the counterjet. The cooling timescale is much shorter than other timescales (Sari, Narayan, & Piran 1996), so we assume an instantaneous emission at the shock front as before. We use a spherical coordinate system (t, r, θ, ϕ) in the lab frame, where the $\theta = 0$ axis points toward the detector and the central engine is located at $r = 0$. The forward jet has a viewing angle $\theta_v > 0$, which the axis of the emission cone makes with the $\theta = 0$ axis, while the counterjet has a viewing angle $\theta_v + \pi$. When the emitting shock front moves radially from $t = t_0$ and $r = r_0$ with the Lorentz factor $\gamma = 1/(1-\beta^2)^{1/2}$, the emissivity for the XRF has a functional form of

$$j'_{\nu'}(\Omega'_d,\ r,\ t) = A(t) f(\nu') \delta(r - r_0 - \beta c(t - t_0)) \times H(\Delta\theta - |\theta - \theta_v|) \times H\left(\cos\phi - \frac{\cos\Delta\theta - \cos\theta_v \cos\theta}{\sin\theta_v \sin\theta}\right), \quad (1)$$

where $f(\nu')$ represents the spectral shape. The Heaviside step function $H(x)$ indicates that the emission is inside a cone of an opening half-angle $\Delta\theta$. Then, the observed flux per unit frequency of a single pulse at the observed time T is given by

$$F_\nu(T) = \frac{2r_0^2\gamma^2}{\beta D^2 (r_0/c\beta)} \times \int dt\, A(t) \frac{\gamma^2[1-\beta\cos\theta(T)]}{\gamma^2[1-\beta\cos\theta(t)]} \frac{\Delta\phi(t) f(\nu\gamma[1-\beta\cos\theta(t)])}{\{\gamma^2[1-\beta\cos\theta(t)]\}^2}, \quad (2)$$

where $1 - \beta\cos\theta(T) = (c\beta/r_0)(T - T_0)$, $1 - \beta\cos\theta(t) = [1 - \beta\cos\theta(T)]/[(c\beta/r_0)(t - T_0)]$, and $T_0 = t_0 - r_0/c\beta$ (see Ioka & Nakamura 2001a). For the XRF, $\theta(t)$ varies from $\max(0,\ \theta_v - \Delta\theta)$ to $\theta_v + \Delta\theta$. The function $\Delta\phi(t)$ is given as

$$\Delta\phi(t) = \begin{cases} \pi\,, & \theta_v < \Delta\theta,\ 0 < \theta(t) \le \Delta\theta - \theta_v\,, \\ \cos^{-1}\left[\dfrac{\cos\Delta\theta - \cos\theta(t)\cos\theta_v}{\sin\theta_v \sin\theta(t)}\right], & \text{otherwise}\,. \end{cases} \quad (3)$$

For the DF also, we can use equation (2). For the DF, $\theta(t)$ varies from $\pi + \max(0,\ \theta_v - \Delta\theta)$ to $\pi + \theta_v + \Delta\theta$, and the function $\Delta\phi(t)$ is given as

$$\Delta\phi(t) = \begin{cases} \pi\,, & \theta_v < \Delta\theta,\ \pi < \theta(t) \le \pi + \Delta\theta - \theta_v\,, \\ \cos^{-1}\left[\dfrac{\cos\Delta\theta + \cos\theta(t)\cos\theta_v}{-\sin\theta_v \sin\theta(t)}\right], & \text{otherwise}\,. \end{cases} \quad (4)$$

The normalization of emissivity $A(t)$ is determined by the hydrodynamics. Here, for simplicity we adopt the following functional form:

$$A(t) = A_0 \left(\frac{t - T_0}{r_0/c\beta}\right)^{-2} H(t - t_0) H(t_e - t)\,, \quad (5)$$

where the emission ends at $t = t_e$ and the released energy at each distance r is constant. Our conclusion does not depend so much on t_e or the functional form. The pulse-starting time and ending time are given as

$$T_{\rm start}^{\rm (XRF)} = T_0 + \frac{r_0}{c\beta}\{1 - \beta\cos[\max(0,\ \theta_v - \Delta\theta)]\}\,, \quad (6)$$

$$T_{\rm end}^{\rm (XRF)} = T_0 + \left(\frac{r_0}{c\beta} + t_e - t_0\right)[1 - \beta\cos(\theta_v + \Delta\theta)] \quad (7)$$

for the XRF, and

$$T_{\rm start}^{\rm (DF)} = T_0 + \frac{r_0}{c\beta}[1 + \beta\cos(\theta_v + \Delta\theta)]\,, \quad (8)$$

$$T_{\rm end}^{\rm (DF)} = T_0 + \left(\frac{r_0}{c\beta} + t_e - t_0\right)\{1 + \beta\cos[\max(0,\ \theta_v - \Delta\theta)]\} \quad (9)$$

for the DF.

The spectrum of the GRB is well approximated by the Band spectrum (Band et al. 1993). In order to have a spectral shape similar to the Band spectrum, we adopt the following form of the spectrum in the comoving frame:

$$f(\nu') = \left(\frac{\nu'}{\nu'_0}\right)^{1+\alpha_{\rm B}} \left(1 + \frac{\nu'}{\nu'_0}\right)^{\beta_{\rm B} - \alpha_{\rm B}}, \quad (10)$$

where $\alpha_{\rm B}$ and $\beta_{\rm B}$ are the low- and high-energy power-law indexes, respectively. In the GRB, $\alpha_{\rm B} \sim -1$ and $\beta_{\rm B} \sim -3$ are typical values (Preece et al. 2000). Equations (2), (5), and (10) are the basic equations to calculate the flux of a single pulse, which depends on the following parameters: $\gamma \gg 1$, $\theta_v \ll 1$, $\Delta\theta \ll 1$, $\gamma\nu'_0$, $r_0/c\beta\gamma^2$, $\alpha_{\rm B}$, $\beta_{\rm B}$, D, A_0, t_0, and t_e.

Hereafter, we consider mainly the following canonical set of parameters: $\gamma = 100$, $\gamma\Delta\theta = 5$, $r_0/\beta c\gamma^2 = 1$ s, $\alpha_{\rm B} = -1$, $\beta_{\rm B} = -3$, $h\gamma\nu'_0 = 200$ keV, and $t_0 = r_0/c\beta$. We adopt $t_e = 1.3 r_0/c\beta$ since most pulses rise more quickly than they decay (Norris et al. 1996). The value $\gamma\Delta\theta = 5$ has been obtained from the fitting of the afterglow light curve (Frail et al. 2001; see also Panaitescu & Kumar 2002). We fix the amplitude A_0 so that the isotropic gamma-ray energy $E_{\rm iso} = 4\pi D^2 S(20\text{–}2000\ {\rm keV})$ satisfies $(\Delta\theta)^2 E_{\rm iso} = 1 \times 10^{51}$ ergs when $\gamma\theta_v = 0$ (Frail et al. 2001). Here $S(\nu_1\text{–}\nu_2) = \int_{T_{\rm start}}^{T_{\rm end}} F(T;\ \nu_1\text{–}\nu_2)\, dT$ is the observed fluence in the energy range $\nu_1\text{–}\nu_2$, and $F(T;\ \nu_1\text{–}\nu_2) = \int_{\nu_1}^{\nu_2} F_\nu(T)\, d\nu$ is the observed flux in the same energy range. Then, we obtain $A_0 = 0.24$ ergs s^{-1} cm^{-2} Hz^{-1} for the fiducial parameters. Note that the observed flux is proportional to D^{-2}.[1]

3. LIGHT CURVES OF THE X-RAY FLASH AND DELAYED FLASH

In this section we plot the light curves of the XRF and the DF using equation (2) and discuss whether these events can be observed by the *Swift* satellite. First, we show the light

[1] When we consider the effect of cosmology ($\Omega_M = 0.3$, $\Omega_\Lambda = 0.7$, and $h = 0.7$), $D \sim 1$ Gpc corresponds to $z \sim 0.2$. Since we consider the case $D < 1$ Gpc in the following sections, this does not affect our argument qualitatively but alters the quantitative results by up to a factor of 2.

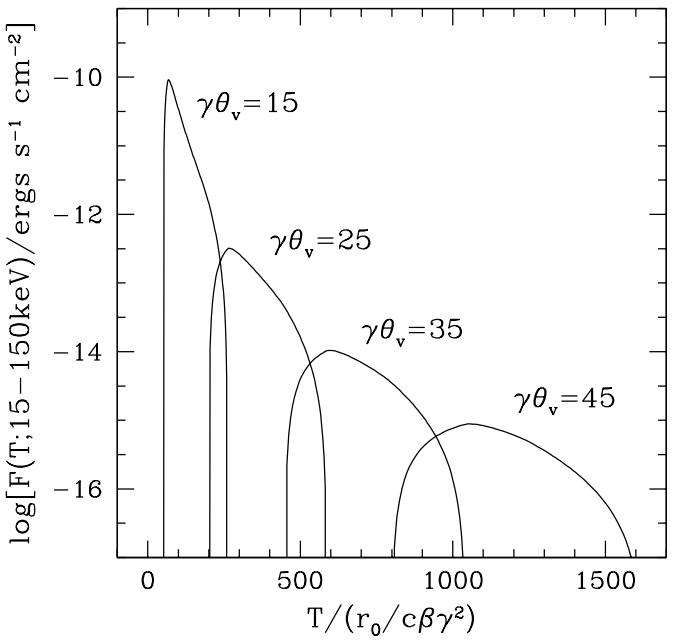

FIG. 1.—Light curves of the XRF as a function of the normalized observed time $T/(r_0/c\beta\gamma^2)$, where we adopt $r_0/\beta c\gamma^2 = 1$ s. We choose $\gamma\Delta\theta = 5$, $\alpha_B = -1$, $\beta_B = -3$, $\gamma\nu'_0 = 200$ keV, and $D = 1$ Gpc. The flux is proportional to D^{-2}.

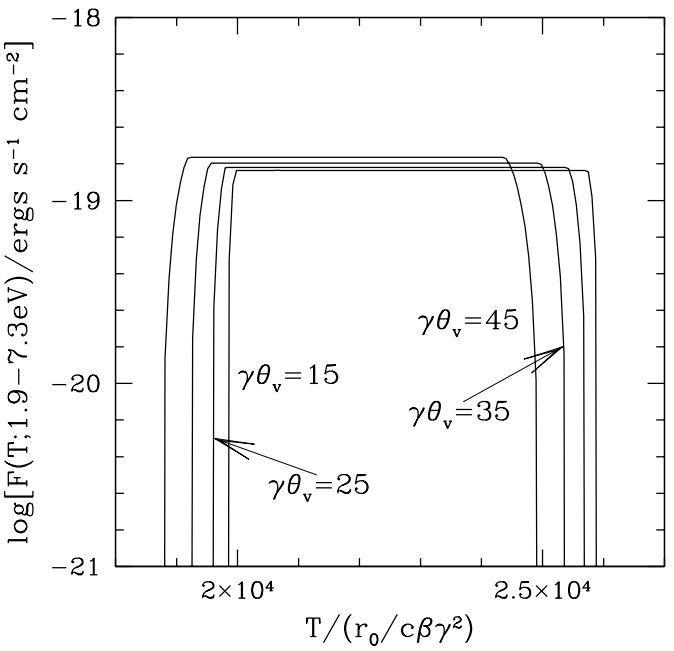

FIG. 2.—Light curves of the DF as a function of the normalized observed time $T/(r_0/c\beta\gamma^2)$, where we adopt $r_0/\beta c\gamma^2 = 1$ s. We choose $\gamma = 100$, $\gamma\Delta\theta = 5$, $\alpha_B = -1$, $\beta_B = -3$, $\gamma\nu'_0 = 200$ keV, and $D = 1$ Gpc. Our jet model predicts that the flux of the DF be almost constant ($F \sim 2 \times 10^{-19} D_{\rm Gpc}^{-2}$ ergs s^{-1} cm^{-2}) with both the observed time and the viewing angle.

curves of the XRF $F(T;$ 15–150 keV) in Figure 1 with varying $\gamma\theta_v$. The observation band corresponds to that of the Burst Alert Telescope (BAT) on *Swift*. As $\gamma\theta_v$ increases, the peak flux of the XRF $F_{\rm peak}^{\rm (XRF)}$ decreases because of the relativistic beaming effect.

The light curves of the DF $F(T;$ 1.9–7.3 eV) are shown in Figure 2 with varying $\gamma\theta_v$. The observation band corresponds that of the Ultraviolet and Optical Telescope (UVOT) on *Swift*. We find that the flux remains almost constant in each pulse and that the peak flux $F_{\rm peak}^{\rm (DF)}$ does not depend so much on the viewing angle $\gamma\theta_v$. This is because the value of $\theta(t)$ ranges between $\pi + \max(0,\ \theta_v - \Delta\theta)$ and $\pi + \theta_v + \Delta\theta$, and $(c\beta/r_0)(t - T_0) \sim 1$ so that $\theta(t) \sim \theta(T) \sim \pi$ in equation (2). From equation (2) the peak flux of the DF can be estimated as $F_{\rm peak}^{\rm (DF)} \sim \Delta\nu F_\nu \sim \Delta\nu(2r_0^2\gamma^2/\beta D^2) A_0\Delta\phi f/(2\gamma^2)^2 \sim 10^{-19}$ ergs s^{-1} cm^{-2}, where $\Delta\nu \sim 10^{14}$ Hz, $\Delta\phi \sim \Delta\theta/\theta_v \sim 0.1$, and $f \sim 0.2$.

The limiting sensitivity of the UVOT can be estimated as 1×10^{-15} ergs s^{-1} cm^{-2} for a duration of $\sim 5 \times 10^3$ s, while that of BAT can be estimated as 5×10^{-10} ergs s^{-1} cm^{-2} for a duration of $\sim 10^2$ s. The BAT localizes the XRF, and the following observation by the UVOT may identify the associated DF. One can see that a DF with $D \lesssim 13$ Mpc is observable. Then, the BAT can detect the preceding XRF if $\gamma\theta_v \lesssim 30$.

4. AFTERGLOW OF THE X-RAY FLASH

The start and end times of the DF are about $T_{\rm start}^{\rm (DF)} \sim 2t_0 \sim 2 \times 10^4$ s and $T_{\rm end}^{\rm (DF)} \sim 2t_e \sim 2.6 \times 10^4$ s for $\gamma = 10^2$, $t_0 = r_0/c\beta = 10^4$ s, and $t_e = 1.3t_0$. Therefore, one should compare the flux of the DF with that of the XRF afterglow. In this section we plot the light curves of the XRF afterglow and see whether or not the DF can be detected. We use model 1 of Granot et al. (2002) as a simple model of the off-axis afterglow emission from the collimated jet (see also Dalal, Griest, & Pruet 2002).

For $\theta_v = 0$, the standard afterglow model, i.e., the synchrotron-shock model, can explain the observational properties of the GRB afterglow very well (Piran 1999) and gives the observed flux per unit frequency as $F_\nu(T;\ \theta_v = 0) = F_\nu^{\rm (R\text{-}SPH)} \equiv G(\nu,\ T)$, where $F_\nu^{\rm (R\text{-}SPH)}$ is the observed flux given by Rhoads (1999) and Sari, Piran, & Halpern (1999). For $\theta_v > \Delta\theta$, the emission is assumed to be from a point source moving along the jet axis. Then, the flux is given by $F_\nu(T;\ \theta_v) = a^3 G(a^{-1}\nu,\ aT)$, where $a \equiv (1 - \beta)/(1 - \beta\cos\tilde{\theta}) \sim [1 + (\gamma\tilde{\theta})^2]^{-1}$. We choose $\tilde{\theta} = \max(0,\ \theta_v - \Delta\theta)$ to make this simple model more realistic (Granot et al. 2002). The Lorentz factor of the shell γ can be determined by

$$\gamma\Delta\theta = \begin{cases} \left(\dfrac{aT}{t_{\rm jet}}\right)^{-3/8}, & aT < t_{\rm jet}\ , \\ \left(\dfrac{aT}{t_{\rm jet}}\right)^{-1/2}, & aT > t_{\rm jet}\ , \end{cases} \tag{11}$$

where $t_{\rm jet} = (1.9 \times 10^4\ {\rm s}) n^{-1/3} (\Delta\theta/0.05)^{8/3} (E/2 \times 10^{54}\ {\rm ergs})^{1/3}$ is the jet-break time observed by an on-axis observer,[2] where E is the isotropic equivalent value of the total energy in the shock. We assume $E = \eta_\gamma^{-1} E_{\rm iso}$ with a constant factor $\eta_\gamma = 0.2$, which is adopted in Frail et al. (2001). Then, we obtain $E = 2 \times 10^{54}$ ergs, and the geometry-corrected total energy in the shock $(\Delta\theta)^2 E/2 = 2.5 \times 10^{51}$ ergs.

Using the above equations, we calculate the light curves of the afterglow. In order to study the dependence on the viewing angle θ_v, we fix the rest of the parameters: the power-law index of accelerated electrons $p = 2.25$, the number density

[2] For simplicity, we assume the relation $t' = R/(4\gamma^2 c)$, where t' and R are the time measured by an on-axis observer and the radius of the shock.

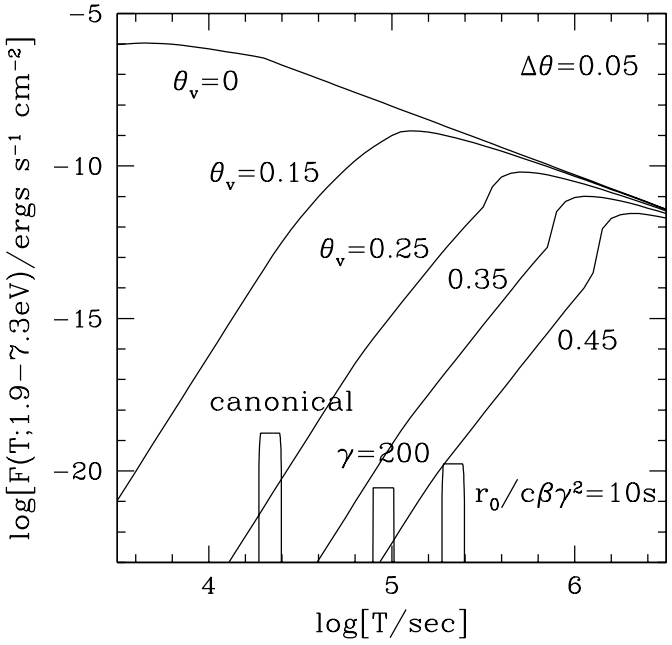

FIG. 3.—Light curves of the XRF afterglow in the UV band, shown by varying the viewing angle θ_v. We fix parameters as $\Delta\theta = 0.05$, $n = 1$ cm^{-3}, $p = 2.25$, $E = 2 \times 10^{54}$ ergs, $\epsilon_e = 0.1$, $\epsilon_B = 0.01$, and $D = 1$ Gpc. Boxes represent the light curves of the DF in the same band. We choose a canonical set of parameters as $\gamma = 100$ and $r_0/\beta c\gamma^2 = 1$ s. The light curve of the DF does not depend so much on the viewing angle θ_v. For comparison, we show the light curves of the DF with one of the fiducial parameters changed. Note that all the flux is proportional to D^{-2}, and the flux and the duration of the DF are proportional to $(r_0/\beta c\gamma^2)^{-1}$ and $r_0/\beta c\gamma^2$, respectively.

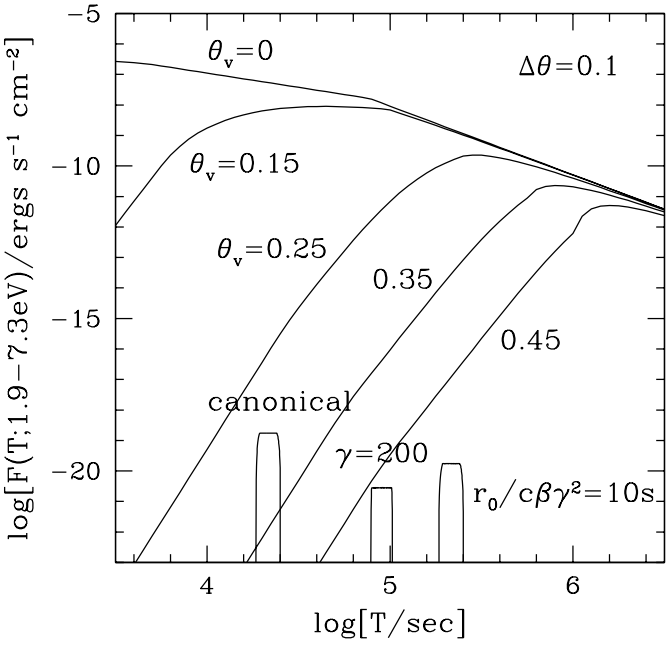

FIG. 4.—Same as Fig. 3, but for $\Delta\theta = 0.1$ and $E = 5 \times 10^{53}$ ergs. Note that the geometry-corrected total energy $(\Delta\theta)^2 E/2$ is not altered.

of the ambient matter $n = 1$ cm^{-3}, $\epsilon_e = 0.1$, $\epsilon_B = 0.01$, and the distance $D = 1$ Gpc. Figure 3 shows the result in the case of $\Delta\theta = 0.05$, and Figure 4 in the case of $\Delta\theta = 0.1$. The observation band is 1.9–7.3 eV, which corresponds to that of UVOT.

We also plot the UV flux of the DF in the same figures. We can see that for the canonical set of parameters ($\Delta\theta = 0.05$, $\gamma = 100$, and $r_0/c\beta\gamma^2 = 1$ s), the UV flux of the DF dominates the afterglow when $\theta_v \gtrsim 0.21$. For comparison, we show the light curves of the DF with one of the parameters changed from the fiducial value. For large γ, it is difficult to detect the DF, since the starting and ending times of the DF are late and the flux of the DF is low because of the strong beaming effect. When we alter $r_0/c\beta\gamma^2$, the starting (and ending) time and the flux of the DF have a dependence $\propto(r_0/c\beta\gamma^2)$ and $\propto(r_0/c\beta\gamma^2)^{-1}$, respectively. Therefore, the large $r_0/c\beta\gamma^2$ case has qualitatively the same behavior as the large-γ case. One can easily find that when $\Delta\theta$ becomes large, the flux of the afterglow of the XRF becomes large, while the light curves of the DF remain almost unchanged. Therefore, we can conclude that the DF from a jet with a smaller $\Delta\theta$, γ, and $r_0/c\beta\gamma^2$ has a larger chance to be seen. In consequence, according to the off-axis jet model, it is preferable for the detection of a DF that the preceding XRF have a low peak energy of a few keV, a small variability owing to large θ_v (Yamazaki, Ioka, & Nakamura 2002a, 2002b), and a short duration due to small $r_0/c\beta\gamma^2$.

We have used in this section model 1 of Granot et al. (2002). A more realistic model for the off-axis emission from the forward jet, model 3 of Granot et al. (2002), may have a more moderate rise before the peak of the observed light curve than the model we have adopted. However, we consider the case in which the viewing angle is as large as $\theta_v \gtrsim 5\Delta\theta$, so that the differences between these models are small.

5. DISCUSSION

We have calculated the light curves of the DF, XRF, and the afterglow of the XRF. We have shown that in principle, the DF emission can be seen in the UV band about 10^4–10^5 s after the XRF if the viewing angle is large enough (about 0.2–0.3 rad) for the afterglow of the XRF to be dimmer than the DF. Since the UV flux of the GRB afterglow is much larger than that of the DF, only the DF associated with an off-axis jet, i.e., an XRF, has any chance to be observed. The preceding XRF should have a low peak energy of a few keV, a small variability, and a short duration for the DF to be detected. Because of the relativistic beaming effect, the flux of the DF is so small that only nearby events ($\lesssim 13$ Mpc for the canonical parameters) can be observed by UVOT on *Swift*. Following Yamazaki, Ioka, & Nakamura (2002a), we can roughly estimate the event rate of the DF for the instruments on *Swift* as $R_{\rm DF} \sim 6 \times 10^{-5}$ events yr^{-1}, where we adopt an event rate of the GRBs $r_{\rm GRB} = 5 \times 10^{-8}$ events yr^{-1} galaxy^{-1} and a number density of galaxies $n_g = 10^{-2}$ galaxies Mpc^{-3}. Therefore, we need next-generation detectors, which will be more sensitive than the instruments on *Swift*, to detect the DFs associated with very dim XRFs more frequently.

The DF may be obscured by dust extinction. In fact, about half of accurately localized GRBs do not produce a detectable optical afterglow (Fynbo et al. 2001; Lazzati, Covino, & Ghisellini 2002). One explanation for these "dark GRBs" is that most GRBs occur in giant molecular clouds (e.g., Reichart & Price 2002). In this picture, a GRB has a detectable optical afterglow only if the burst and the afterglow destroy the dust along the line of sight to the observer (Waxman & Draine 2000; Fruchter, Krolik, &

Rhoads 2001), as suggested by the comparison between X-ray and optical extinction (Galama & Wijers 2001). In this case the DF is obscured since the flux of the XRF is too dim to carve out a path for the DF. However, this picture may have some problems, such as no evidence of an ionized absorber (Piro et al. 2002) and variable column density in the X-ray afterglow (Djorgovski et al. 2001a). There are other explanations for dark GRBs, such as high-redshift effects, dust extinction in the interstellar medium of the host galaxy (Ramirez-Ruiz, Trentham, & Blain 2002; Piro et al. 2002), and so on. Therefore, at present we cannot conclude that the DF is obscured.

If we assume that the absolute magnitude of the host galaxy is about -20 mag (Djorgovski et al. 2001b, 2002), the apparent magnitude is about $20 + 5 \log D_{\rm Gpc}$. Since a host galaxy with a size of $\sim$10 kpc has an angular size of $\sim 10 D_{\rm Gpc}^{-1}{}''$, we can observe a point source that is dimmer than the host galaxy by $\sim 10^{-4} D_{\rm Gpc}^{2}$ if the angular resolution is $\sim 0''.1$. Therefore, the DF has to be brighter than $\sim$30 mag, and we can observe the DF if $D \lesssim 13$ Mpc.

If the GRB is associated with a supernova (SN), the emission from the SN may hide the DF. The UV flux of SN 1998bw was about $\sim$17 mag at the distance $D \sim 40$ Mpc (Galama et al. 1998), i.e., $\sim 6 \times 10^{-15} D_{\rm Gpc}^{-2}$ ergs s^{-1} cm^{-2}, so a SN such as SN 1998bw is brighter than the DF. However, at present it is not clear whether all GRBs are associated with SNe or not (e.g., Price et al. 2003). In any case, deep searches following the XRF will give us valuable information.

If the DF associated with an XRF is observed, we will be able to estimate the Lorentz factor and the viewing angle of the jets. Let the typical frequency or the break energy of the DF be $\nu_{\rm DF} = \delta_{\rm DF} \nu'_0$, or $\nu_{\rm XRF} = \delta_{\rm XRF} \nu'_0$ for the XRF, where $\delta \equiv 1/\gamma(1 - \beta \cos \theta_v)$ is the Doppler factor. When $\theta_v \ll 1$, $\gamma \gg 1$, and $(\gamma \theta_v)^2 \gg 1$, we can derive $\delta_{\rm DF} \sim 1/(2\gamma)$ and $\delta_{\rm XRF} \sim 2\gamma/(\gamma\theta_v)^2$. Since we assume that the XRF is a GRB observed from an off-axis viewing angle, we can assume a typical observed photon energy of $\delta_{\rm GRB} h\nu'_0 \sim 200\xi$ keV, where $\xi \sim 0.5$–2 (Preece et al. 2000). In our model, $\delta_{\rm GRB}$ becomes $\sim 2\gamma$. Then, we obtain $\gamma \sim 100 \xi^{1/2} (h\nu_{\rm DF}/5\ {\rm eV})^{-1/2}$. On the other hand, we can derive $\nu_{\rm DF}/\nu_{\rm XRF} \sim (\theta_v/2)^2$, which implies that we can also estimate the viewing angle.

We would like to thank the referee for useful comments and suggestions. We are grateful to A. Yoshida and T. Murakami for helpful comments and W. Naylor for a careful reading of the manuscript. This work was supported in part by Grants-in-Aid 00660 (K. I.), 14047212 (T. N.), and 14204024 (T. N.) for Scientific Research of the Japanese Ministry of Education, Culture, Sports, Science, and Technology.

REFERENCES

Band, D., et al. 1993, ApJ, 413, 281
Barraud, C., et al. 2003, A&A, 400, 1021
Begelman, M. C., Blandford, R. D., & Rees, M. J. 1984, Rev. Mod. Phys., 56, 255
Dado, S., Dar, A., & De Rújula, A. 2002, A&A, 388, 1079
Dalal, N., Griest, K., & Pruet, J. 2002, ApJ, 564, 209
Djorgovski, S. G., Frail, D. A., Kulkarni, S. R., Bloom, J. S., Odewahn, S. C., & Diercks, A. 2001a, ApJ, 562, 654
Djorgovski, S. G., et al. 2001b, in Proc. Gamma-Ray Bursts in the Afterglow Era, ed. E. Costa, F. Frontera, & J. Hjorth (Berlin: Springer), 218
———. 2002, in Proc. IX Marcel Grossmann Meeting, ed. V. Gurzadyan, R. Jantzen, & R. Ruffini (Singapore: World Scientific), 315
Frail, D. A., et al. 2001, ApJ, 562, L55
Fruchter, A., Krolik, J. H., & Rhoads, J. E. 2001, ApJ, 563, 597
Fynbo, J. U., et al. 2001, A&A, 369, 373
Galama, T. J., & Wijers, R. A. M. 2001, ApJ, 549, L209
Galama, T. J., et al. 1998, Nature, 395, 670
Ghisellini, G., & Lazzati, D. 1999, MNRAS, 309, L7
Granot, J., Panaitescu, A., Kumar, P., & Woosley, S. E. 2002, ApJ, 570, L61
Heise, J., in 't Zand, J., Kippen, R. M., & Woods, P. M. 2001, in Proc. Gamma-Ray Bursts in the Afterglow Era, ed. E. Costa, F. Frontera, & J. Hjorth (Berlin: Springer), 16
Huang, Y. F., Dai, Z. G., & Lu, T. 2002, MNRAS, 332, 735
Ioka, K., & Nakamura, T. 2001a, ApJ, 554, L163
———. 2001b, ApJ, 561, 703
Kippen, R. M., Woods, P. M., Heise, J., in 't Zand, J. J. M., Briggs, M. S., & Preece, R. D. 2003, in Proc. Woods Hole Gamma-Ray Burst Workshop, ed. R. Vanderspek (New York: AIP), in press
Lazzati, D., Covino, S., & Ghisellini, G. 2002, MNRAS, 330, 583
Meikle, W. P. S., et al. 1987, Nature, 329, 608
Mirabel, I. F., & Rodríguez, L. F. 1999, ARA&A, 37, 409
Nakamura, T. 2000, ApJ, 534, L159
Nisenson, P., & Papaliolios, C. 1999, ApJ, 518, L29
Nisenson, P., et al. 1987, ApJ, 320, L15
Norris, J. P., et al. 1996, ApJ, 459, 393
Panaitescu, A., & Kumar, P. 2002, ApJ, 571, 779
Piran, T. 1999, Phys. Rep., 314, 575
Piran, T., & Nakamura, T. 1987, Nature, 330, 28
Piro, L., et al. 2002, ApJ, 577, 680
Preece, R. D., Briggs, M. S., Mallozzi, R. S., Pendleton, G. N., Paciesas, W. S., & Band, D. L. 2000, ApJS, 126, 19
Price, P. A., et al. 2003, ApJ, 584, 931
Ramirez-Ruiz, E., Trentham, N., & Blain, A. W. 2002, MNRAS, 329, 465
Rees, M. J. 1987, Nature, 328, 207
Reichart, D. E., & Price, P. 2002, ApJ, 565, 174
Rhoads, J. E. 1999, ApJ, 525, 737
Sari, R. 1999, ApJ, 524, L43
Sari, R., Narayan, R., & Piran, T. 1996, ApJ, 473, 204
Sari, R., Piran, T., & Halpern, J. P. 1999, ApJ, 519, L17
Totani, T., & Panaitescu, A. 2002, ApJ, 576, 120
Wang, L., et al. 2002, ApJ, 579, 671
Waxman, E., & Draine, B. T. 2000, ApJ, 537, 796
Yamazaki, R., Ioka, K., & Nakamura, T. 2002a, ApJ, 571, L31
———. 2002b, ApJ, submitted (astro-ph/0212557)